Cluster Growth Reactions with Selenido-Carbonyl Clusters − Synthesis, Characterisation and Theoretical Study of the Dimetallic *closo* Clusters $[WRu_3(\mu_4\text{-}Se)_2(\mu\text{-}CO)_4(CO)_6(L)_2]$ (L = Phosphane) and of the Donor-Acceptor Adduct $[(CO)_5W(\mu_4\text{-}Se)Ru_3(\mu_3\text{-}Se)(CO)_7\{P(CH_2Ph)Ph_2\}_2]$

Daniele Cauzzi,[a] Claudia Graiff,[a] Roberto Pattacini,[a] Giovanni Predieri,*[a] Antonio Tiripicchio,[a] Samia Kahlal,[b] and Jean-Yves Saillard[b]

Keywords: Ruthenium / Tungsten / Molybdenum / Cluster compounds / Selenium

The open-triangular, *nido* clusters of the type $[Ru_3(\mu_3\text{-}Se)_2(CO)_7(L)_2]$ (L = PPh_3, $PPh_2(OMe)$, $PPh_2(Me)$, $P(p\text{-}MeOC_6H_4)_3$] react at room temperature with $[W(CO)_3(MeCN)_3]$ to give the dimetallic *closo* clusters $[WRu_3(\mu_4\text{-}Se)_2(\mu\text{-}CO)_4(CO)_6(L)_2]$. When L is $P(CH_2Ph)Ph_2$ the donor-acceptor adduct $[(CO)_5W(\mu_4\text{-}Se)Ru_3(\mu_3\text{-}Se)(CO)_7\{P(CH_2Ph)Ph_2\}_2]$ is obtained where the *nido* cluster $[Ru_3(\mu_3\text{-}Se)_2(CO)_7(L)_2]$ interacts with the fragment $W(CO)_5$ through a selenido ligand. DFT calculations, performed on the model species $[WRu_3(\mu_4\text{-}Se)_2(\mu\text{-}CO)_4(CO)_6(PH_3)_2]$ and $[(CO)_5W(\mu_4\text{-}Se)Ru_3(\mu_3\text{-}Se)(CO)_7(PH_3)_2]$, showed that the computed total energy of the latter is 1.1 eV lower than that of the former.

Introduction

In recent years we have carried out systematic investigations on the selenium-transfer reactions of tertiary phosphane and diphosphane selenides with carbonyl clusters $M'_3(CO)_{12}$ (M′ = Fe or Ru).[1−9] These reactions take advantage of the frailty of the P=Se bond and provide a simple, sometimes selective,[2] synthetic route to phosphane-substituted, mono- and diselenido clusters. When the starting phosphane contains heterocyclic groups, such as the 2-pyridyl and 2-thienyl moieties, P−C bond cleavage is observed, affording selenido-phosphido clusters coordinating to heterocyclic fragments.[5−7]

The synthesis of phosphane-substituted mixed-metal selenido clusters has also been investigated as the presence of different metals can influence the selectivity of certain processes,[8,9] leading to the formation of compounds with new and not always easily predictable structures. For the synthesis of dimetallic substituted selenido-carbonyl clusters two different synthetic strategies have been developed: (a) M′M + PSe, i.e. reactions between preformed dimetallic clusters and tertiary phosphane selenides,[10] and (b) M′Se + M, i.e. cluster growth reactions between preformed chalcogenide metal clusters and suitable organometallic fragments.

As regards route (b), selenido clusters $[Ru_3(\mu_3\text{-}Se)_2(CO)_7(L)_2]$ were considered to be ideal candidates for growth reactions. These starting compounds are open-triangular, *nido* clusters with seven skeletal electron pairs (SEPs), according to the requirements of the polyhedral skeletal electron pair (PSEP) theory. As a consequence they could be prone to add a zero SEP fragment, such as $M(CO)_3$, derived from $[M(CO)_3(CH_3CN)_3]$ (M = Mo or W), giving the corresponding *closo* clusters $[MRu_3(\mu_4\text{-}Se)_2(CO)_{10}(L)_2]$. In this regard Adams[11] and co-workers obtained the monophosphane sulfur derivative of formula $[WRu_3(\mu_4\text{-}S)_2(CO)_{11}(PMe_2Ph)]$ upon irradiating a solution of $[Ru_3(\mu_3\text{-}S)_2(CO)_9]$ and $[W(CO)_5(PMe_2Ph)]$.

In a preliminary communication,[12] the products of the reactions between $[Ru_3(\mu_3\text{-}Se)_2(CO)_7(PPh_3)_2]$ and $[M(CO)_3(CH_3CN)_3]$ were erroneously identified as the unexpected, centrosymmetric *closo* clusters $[M_2Ru_2(\mu_4\text{-}Se)_2(\mu\text{-}CO)_4(CO)_6(PPh_3)_2]$ (M = W or Mo) on the basis of misinterpreted X-ray structural analyses. However, preliminary MO calculations, mass spectral and accurate elemental analysis data stimulated further crystallographic studies, which revealed that a disorder exists in the crystals of these compounds involving the mutually opposite Ru and W atoms of the *closo* core of the cluster. This results in a disordered $Ru_3M(\mu_4\text{-}Se)_2$ cluster core instead of a centrosymmetric $M_2Ru_2(\mu_4\text{-}Se)_2$ one. Definitive evidence for this was provided by the solution of the crystal structure of $[WRu_3(\mu_4\text{-}Se)_2(\mu\text{-}CO)_4(CO)_6\{P(OMe)Ph_2\}_2]$ which does not

[a] Dipartimento di Chimica Generale ed Inorganica, Chimica Analitica, Chimica Fisica, Università di Parma,
Parco Area delle Scienze 17/A, 43100 Parma, Italy
Fax: (internat.) + 39-0521/905-557
E-mail: predieri@unipr.it
[b] LCSIM-UMR 6511, Institut de Chimie de Rennes, Université de Rennes 1,
35042 Rennes-Cedex, France

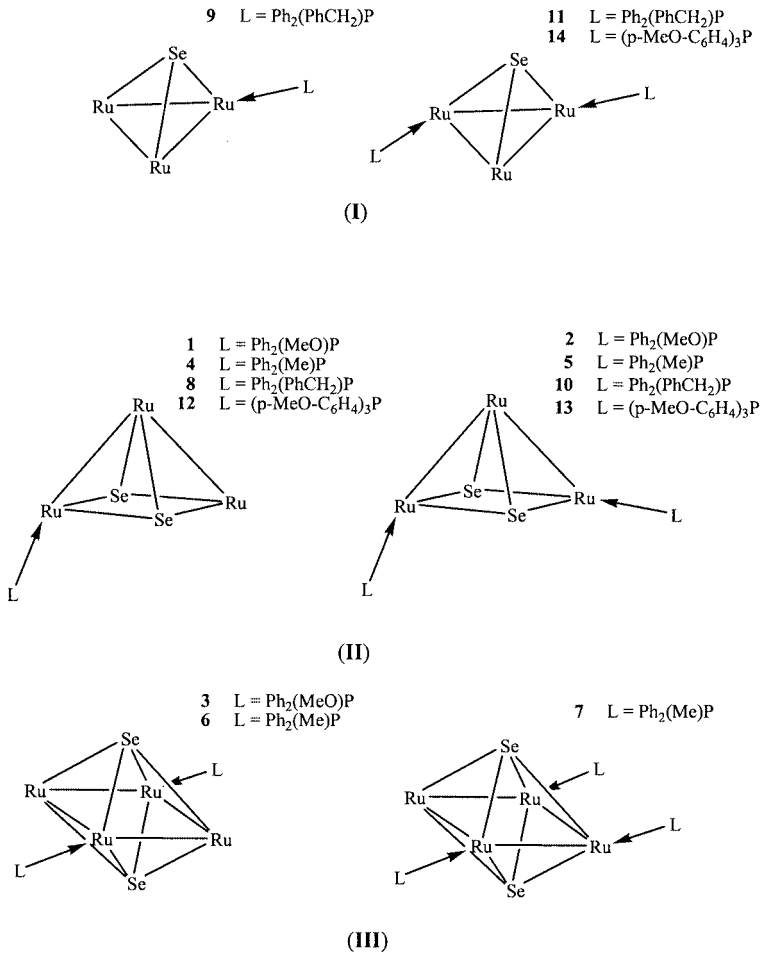

Scheme 1. (Carbonyl groups omitted)

exhibit the disorder described above. Consequently, this paper deals with the synthesis of five $[MRu_3(\mu_4\text{-}Se)_2(\mu\text{-}CO)_4(CO)_6(L)_2]$ clusters [M = Mo, L = PPh_3; M = W, L = $PPh_2(Me)$, $PPh_2(OMe)$, $P(p\text{-}MeO\text{-}C_6H_4)_3$] and the structural characterisation of four of them. In the case of the reaction involving $P(CH_2Ph)Ph_2$, we obtained $[(CO)_5W(\mu_4\text{-}Se)Ru_3(\mu_3\text{-}Se)(CO)_7\{P(CH_2Ph)Ph_2\}_2]$, which can be considered as the product of a donor-acceptor interaction between $[Ru_3(\mu_3\text{-}Se)_2(CO)_7\{P(CH_2Ph)Ph_2\}_2]$ and the $W(CO)_5$ fragment through a selenido ligand. Moreover, DFT calculations have been performed on the model compounds $[WRu_3(\mu_4\text{-}Se)_2(\mu\text{-}CO)_4(CO)_6(PH_3)_2]$ and $[(CO)_5W(\mu_4\text{-}Se)Ru_3(\mu_3\text{-}Se)(CO)_7(PH_3)_2]$. Besides these major results, some new phosphane selenides have been characterised, and used to produce the selenido clusters shown in Scheme 1. They can be grouped in three different families according to the cluster cores: Ru_3Se (I), Ru_3Se_2 (II) and Ru_4Se_2 (III). The crystal structures of two of them, $[Ru_3(\mu_3\text{-}Se)_2(CO)_7(L)_2]$ [L = $PPh_2(OMe)$ or $P(CH_2Ph)Ph_2$], have been determined by X-ray methods.

Results and Discussion

The new tertiary phosphane selenides $Ph_2(Me)PSe$, $Ph_2(MeO)PSe$, $(p\text{-}MeOC_5H_4)_3PSe$ and $Ph_2(PhCH_2)PSe$ were obtained in quantitative yield by selenium transfer from elemental Se to the parent phosphane. They exhibit a characteristic P=Se IR stretching band in the range 520−530 cm^{-1} and a ^{31}P NMR signal with ^{77}Se satellites, $^1J_{P,Se}$ being in the range 710−740 Hz as normally found in similar species.[13]

The reaction between $[Ru_3(CO)_{12}]$ and the tertiary phosphane selenides in hot toluene and in the presence of Me_3NO gave a number of substituted selenidoruthenium carbonyl clusters (some of them, **8**−**14**, already known) belonging to three different families: the monoselenido trinuclear species with a $Ru_3(\mu_3\text{-}Se)$ core (**9**, **11**, **14**; type I), the diselenido trinuclear species with a $Ru_3(\mu_3\text{-}Se)_2$ core (**1**, **2**, **4**, **5**, **8**, **10**, **12**, **13**; type II), and the diselenido tetranuclear species with a $Ru_4(\mu_4\text{-}Se)_2$ core (**3**, **6**, **7**; type III. See Scheme 1). As the reaction conditions are the same for all phosphanes, it appears that the product distribution is influenced by the nature of the phosphane.

Clusters belonging to the type I family could be regarded as the primary product of the attack of one molecule of the phosphane selenide on the starting reagent $[Ru_3(CO)_{12}]$, resulting in the transfer of a selenium atom to the metal triangle and the substitution of one or two carbonyl groups. These clusters undergo a second attack by another phos-

phane selenide molecule affording, under appropriate conditions, the corresponding diselenido derivatives (clusters of type II). Mono- and disubstituted diselenido species are always present even if the starting Ru_3/PSe molar ratio is 1:1. Type II clusters can be described as square pyramids with two ruthenium and two selenium atoms alternating in the basal plane and the third ruthenium atom at the apex of the pyramid. Mono- and disubstitution by phosphanes occurs only at the base of the pyramid.

Type III clusters belong to the family of tetranuclear *closo* clusters with seven SEPs. They can be described as octahedral clusters with four ruthenium atoms in the equatorial plane and two selenium atoms at the apices. Two (**3**, **6**) or three (**7**) phosphane ligands substitute the same number of carbonyl groups. The coordination around each ruthenium atom is completed by carbonyl groups.

Slow crystallisation of compounds **2** and **10** from dichloromethane solutions afforded well-formed crystals suitable for an X-ray diffraction analysis. ORTEP views of **2** and **10** are shown in Figure 1 and 2, respectively. The most important bond lengths and angles are given in Table 1 together with those of a cluster of formula $[Ru_3(\mu_3\text{-Se})_2(CO)_7(PPh_3)_2]$.[2]

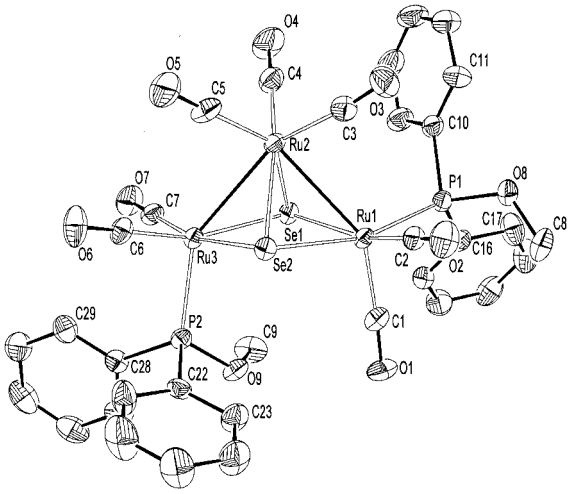

Figure 1. View (ORTEP, 30% probability level) of the molecular structure of **2** with the atom numbering scheme

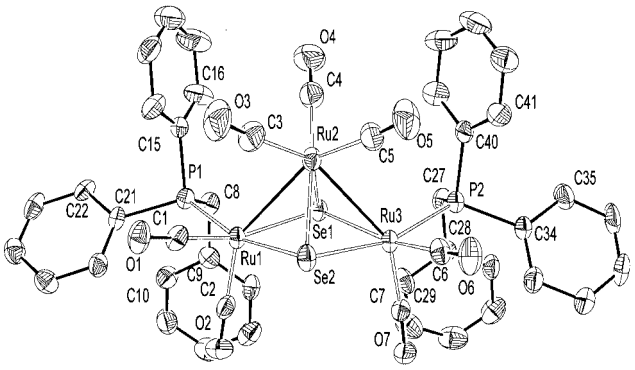

Figure 2. View (ORTEP, 30% probability level) of the molecular structure of **10** with the atom numbering scheme

The cluster cores are similar to that of the analogous compound $[Ru_3(\mu_3\text{-Se})_2(CO)_7(PPh_3)_2]$[2] in which the Ru−Ru bond lengths are 2.801(2) and 2.855(2) Å; those of the six Ru−Se bonds range from 2.491(1) to 2.536(2) Å. The Ru−Ru bond lengths are 2.831(2) and 2.847(2) Å in **2** and 2.799(2) and 2.806(2) Å in **10**, whereas the Ru−Se bond lengths range from 2.485(1) to 2.529(2) Å in **2** and from 2.449(2) to 2.500(2) Å in **10**. In **10** the two diphenylbenzylphosphane ligands coordinate to two ruthenium atoms, substituting two carbonyl groups in *pseudo*-equatorial positions [the P1−Ru1 and P2−Ru3 bond lengths are 2.309(2) and 2.306(3) Å]. In **2** the two diphenylmethoxyphosphane ligands substitute two carbonyls in a *pseudo*-equatorial and *pseudo*-axial position. The P1−Ru1 and P2−Ru3 bond lengths [2.327(2) and 2.274(3) Å] differ remarkably because of the different *trans* influence of the Ru−Ru and Ru−Se bonds.

Clusters **2** and **10** show the same NMR behaviour in solution despite the different coordination of the phos-

Table 1. Comparison of selected bond lengths (Å) and angles (°) for compounds **2**, **10** and $[Ru_3(\mu_3\text{-Se})_2(CO)_7(PPh_3)_2]$

	2	**10**	$[Ru_3(\mu_3\text{-Se})_2(CO)_7(PPh_3)_2]$
Ru(1)−Ru(2)	2.8312(15)	2.8061(15)	2.855(2)
Ru(2)−Ru(3)	2.847(2)	2.7991(17)	2.801(2)
Ru(1)−Se(1)	2.4853(12)	2.4491(16)	2.514(2)
Ru(1)−Se(2)	2.5143(15)	2.4761(16)	2.491(2)
Ru(2)−Se(1)	2.5240(12)	2.4757(18)	2.523(2)
Ru(2)−Se(2)	2.5290(15)	2.500(2)	2.536(2)
Ru(3)−Se(1)	2.4872(16)	2.4497(15)	2.514(2)
Ru(3)−Se(2)	2.4987(12)	2.4704(16)	2.505(2)
Ru(1)−P(1)	2.327(2)	2.309(2)	2.371(4)
Ru(3)−P(2)	2.274(2)	2.306(3)	2.326(3)
Ru(1)−Ru(2)−Ru(3)	83.59(5)	83.96(6)	85.6(1)
Se(1)−Ru(3)−Se(2)	80.98(4)	80.30(6)	79.4(1)
Se(1)−Ru(1)−Se(2)	80.71(4)	80.20(6)	79.7(1)
Se(1)−Ru(2)−Se(2)	79.69(5)	79.23(7)	78.7(1)
Ru(1)−Se(1)−Ru(3)	99.11(4)	99.87(6)	100.6(1)
Ru(3)−Se(2)−Ru(1)	98.03(4)	98.56(6)	99.7(1)

phane ligands in the solid state (eq-ax and eq-eq respectively). The room temperature ^{31}P NMR spectra of clusters **2** and **10**, as well as **5** and **13**, show two broad peaks which collapse at a temperature higher than 40 °C, together with two sharp singlets (see Figure 3 for **13**).

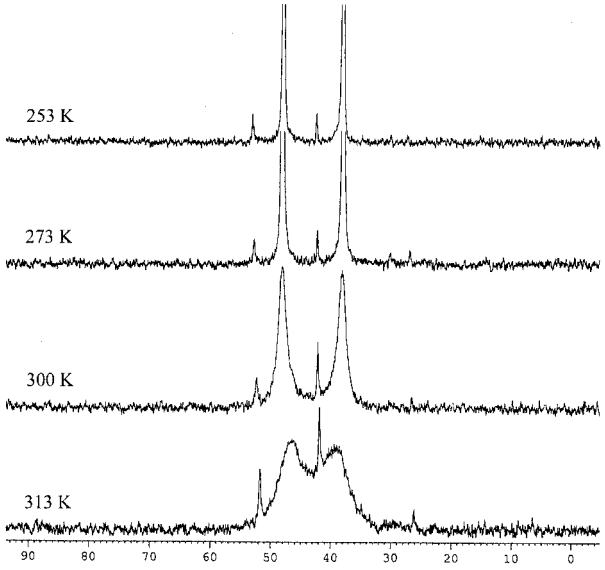

Figure 3. $^{31}P\{^1H\}$ NMR spectra of compound **13** recorded at different temperatures evidencing the incipient coalescence of the broad signals due to the different coordination modes of the phosphane ligands; the presence of four signals confirms the existence of the two isomeric forms A (broad peaks) and B (sharp peaks) depicted in Scheme 2

The two sets of peaks suggest the existence of two isomers A and B, indicated below in Scheme 2, as observed for $[Ru_3(\mu_3\text{-}Se)_2(CO)_7(\mu\text{-dppm})]$ (dppm = $Ph_2PCH_2PPh_2$).[14] They should be involved in an exchange process as occurs for the dppm derivative, consisting of the migration of a Ru−Ru bond from one side of the open Ru_3 triangle to the basal plane of the square pyramid (see Scheme 2). For all these complexes, an equilibrium takes place in solution starting from pure crystals of isomers A. The prevalence of isomer A (broader peaks) in solution is suggested by the fact that the basal metal sites are the preferred ones for phosphane substitution.[1] For both isomers the presence of two peaks suggests that the two P ligands are not equivalent. In fact, in B the two phosphanes occupy two different Ru sites, whereas in A (where the two Ru sites are equivalent) the presence of two peaks is probably the consequence of the fact that one phosphane ligand is coordinated in an axial position and the other in an equatorial position. As one ligand moves from the axial to the equatorial position, the other moves from equatorial to axial. This concerted movement of both ligands is responsible for the observed broadening of the major peaks.

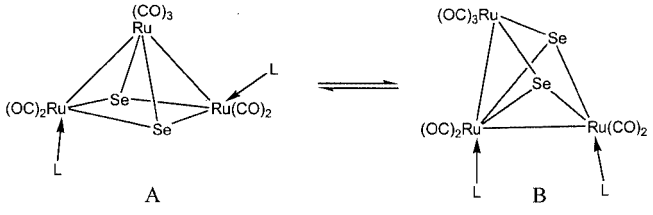

Scheme 2

Cluster Growth Reactions

Type II compounds are open-triangular, *nido* clusters with seven SEPs, according to the PSEP rules. As a consequence they could be prone to add a zero SEP fragment, such as $M(CO)_3$ (M = Mo or W), giving the *closo* clusters $MRu_3(\mu_4\text{-}Se)_2(CO)_{10}(L)_2$. We reacted clusters **2**, **5**, **10** and **13** with an excess of $W(CO)_3(CH_3CN)_3$ in dichloromethane. The reactions take place in a few hours, at room temperature, giving compounds $[WRu_3(\mu_4\text{-}Se)_2(\mu\text{-}CO)_4(CO)_6\{P(OMe)Ph_2\}_2]$ (**15**), $[WRu_3(\mu_4\text{-}Se)_2(\mu\text{-}CO)_4(CO)_6\{P(Me)Ph_2\}_2]$ (**16**), $[WRu_3(\mu_4\text{-}Se)_2(\mu\text{-}CO)_4(CO)_6\{P(p\text{-}MeOC_6H_4)_3\}_2]$ (**17**) and $[(CO)_5W(\mu_4\text{-}Se)Ru_3(\mu_3\text{-}Se)(CO)_7\{P(CH_2Ph)Ph_2\}_2]$ (**20**) as the only isolable products. The IR spectra of **15**−**17**, in the carbonyl region are superimposable with $[WRu_3(\mu_4\text{-}Se)_2(\mu\text{-}CO)_4(CO)_6(PPh_3)_2]$ (**18**) and $[MoRu_3(\mu_4\text{-}Se)_2(\mu\text{-}CO)_4(CO)_6(PPh_3)_2]$ (**19**), suggesting the same molecular structure for all five compounds.

Clusters **15**, **17**, **18** and **19** were unequivocally identified by X-ray diffraction methods (**18** and **19** are isomorphous). Three of these clusters, namely **17**, **18** and **19**, show a crystallographically imposed C_i symmetry, so the mutually opposite Ru and M (M = W or Mo) atoms of the *closo* core of the cluster must be disordered and distributed in the two positions with the same occupancy factor in such a way that a disordered $[Ru_3M(\mu_4\text{-}Se)_2]$ cluster core forms instead of a centrosymmetric $[M_2Ru_2(\mu_4\text{-}Se)_2]$ core. Differently from the clusters **17**, **18** and **19**, cluster **15** does not show this type of disorder.

The structural diagrams of clusters **15**−**20** are shown in Scheme 3.

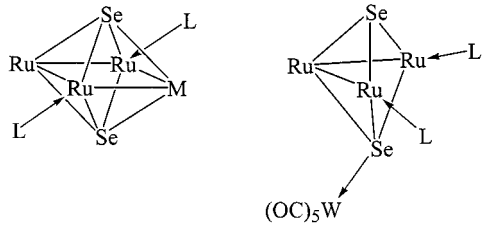

15 L = $P(OMe)Ph_2$ M = W
16 L = $P(Me)Ph_2$ M = W
17 L = $P(p\text{-}MeO\text{-}C_6H_4)_3$ M = W
18 L = PPh_3 M = W
19 L = PPh_3 M = Mo
20 L = $P(CH_2Ph)Ph_2$

Scheme 3. (Carbonyl groups omitted)

Because of the disorder, compounds **18** and **19** were previously identified as the six SEP species $[M_2Ru_2(\mu_4\text{-}Se)_2(\mu\text{-}CO)_4(CO)_6(L)_2]$ (M = W or Mo).[12] According to the PSEP theory, the observed *closo* arrangement is predicted to be unstable for electron-deficient species. This was con-

firmed by DFT calculations on the isoelectronic models $[Mo_2Ru_2(\mu_4\text{-}Se)_2(\mu\text{-}CO)_4(CO)_6(L)_2]$ (L = CO, PH_3) assuming the observed *closo* architecture (geometry optimisation carried out assuming C_{2h} and C_i symmetry for L = CO and PH_3, respectively). Indeed, small HOMO-LUMO gaps were computed for these models (0.24 and 0.44 eV for L = CO and PH_3, respectively). Consistently, the excited triplet state was found to lie close to the singlet ground state (by 0.12 eV and 0.26 eV for L = CO and PH_3, respectively). All these results are indicative of a thermal and kinetic instability for $[M_2Ru_2(\mu_4\text{-}Se)_2(\mu\text{-}CO)_4(CO)_6(L)_2]$ (M = W or Mo), a result at variance with the behaviour of **18** and **19**. On the other hand, calculations on $[Mo_2Ru_2(\mu_4\text{-}Se)_2(\mu\text{-}CO)_4(CO)_6(L)_2]^{2-}$ and $[Mo_2Ru_2(\mu_4\text{-}SeH)_2(\mu\text{-}CO)_4(CO)_6(L)_2]$ (L = CO, PH_3) indicated thermal stability for the regular seven SEP count (HOMO-LUMO gap 1.92 eV (L = CO) and 1.81 eV (L = PH_3) for the former and 1.69 eV (L = CO) and 1.61 eV (L = PH_3) for the latter). Consistently, further crystallographic studies revealed that the correct formula for **18** and **19** is $[MRu_3(\mu_4\text{-}Se)_2(\mu\text{-}CO)_4(CO)_6(L)_2]$ (M = W or Mo).

ORTEP views of **15**, **17**, **18** and **19** are shown in Figure 4, 5, 6 and 7, respectively. The most important bond lengths and angles are given in Table 2 together with those calculated for the complex $[WRu_3(\mu_3\text{-}Se)_2(CO)_{10}(PH_3)_2]$.

The four *closo* seven SEP complexes can be described as distorted octahedra in which the three ruthenium and the M atoms lie in the basal plane with two selenium atoms at the apices. The Ru−Ru bond lengths span from 2.676(7) to 2.835(1) Å. The M−Ru bond lengths range from 2.852(6) to 2.939(2) Å for M = W and from 2.938(8) to 3.027(5) Å for M = Mo. Two phosphane ligands coordinate two nonbonded ruthenium through the phosphorus atoms. Four carbonyls asymmetrically bridge the Ru−Ru and Ru−M edges. The coordination around each metal atom is completed by terminal carbonyl groups.

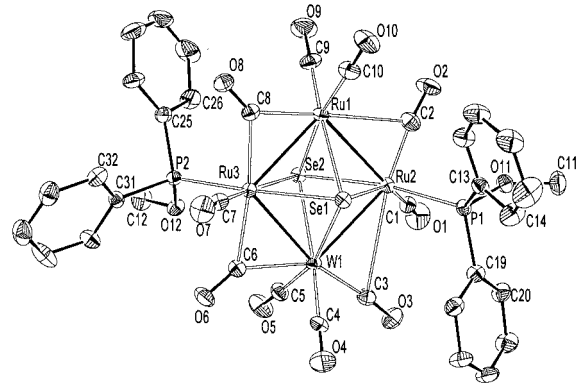

Figure 4. View (ORTEP, 30% probability level) of the molecular structure of **15** with the atom numbering scheme

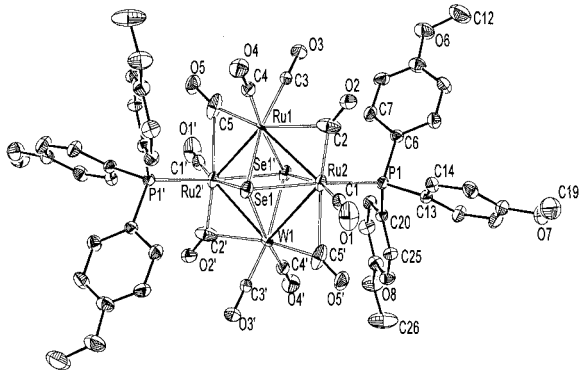

Figure 5. View (ORTEP, 30% probability level) of the molecular structure of one of the two disordered complexes **17** with the atom numbering scheme

DFT calculations on the $[WRu_3(\mu_4\text{-}Se)_2(\mu\text{-}CO)_4(CO)_6(PH_3)_2]$ model (assuming C_1 symmetry) lead to a large HOMO-LUMO gap (1.65 eV), as expected for a *closo*

Table 2. Comparison of selected bond lengths (Å) and angles (°) found for compounds **15**, **17**, **18**, **19** and calculated for complex $[WRu_3(\mu_3\text{-}Se)_2(CO)_{10}(PH_3)_2]$

	15	**17**	**18**	**19**	$WRu_3(\mu_3\text{-}Se)_2(CO)_{10}(PH_3)_2$
Ru(1)−Ru(2)	2.8349(11)	2.792(10)	2.826(4)	2.720(5)	2.878
Ru(1)−Ru(2′)[a]	2.7894(16)	2.676(7)	2.792(3)	2.781(7)	2.870
Ru(2)−M(1)[b]	2.9399(16)	2.935(4)	2.814(2)	2.938(8)	2.940
Ru(2′)−M(1)	2.8639(9)	2.851(6)	2.855(2)	3.027(5)	2.992
M(1)−Se(1)	2.6736(13)	2.658(5)	2.614(3)	2.855(5)	2.775
M(1)−Se(1′)	2.7028(10)	2.679(5)	2.626(2)	2.729(8)	2.775
Ru(1)−Se(1)	2.5841(13)	2.512(9)	2.614(4)	2.581(7)	2.650
Ru(1)−Se(1′)	2.540(4)	2.5894(10)	2.569(4)	2.505(5)	2.620
Ru(2)−Se(1)	2.6196(14)	2.5967(14)	2.5793(14)	2.5782(17)	2.686
Ru(2′)−Se(1′)	2.5878(14)	2.5967(14)	2.5793(14)	2.5782(17)	2.686
Ru(2)−Se(1′)	2.6067(13)	2.5894(10)	2.5976(15)	2.5971(17)	2.685
Ru(2′)−Se(1)	2.5644(11)	2.5894(10)	2.5976(15)	2.5971(17)	2.685
Ru(1)−Ru(2)−M(1)	90.29(4)	87.46(19)	90.73(8)	94.2(2)	92
Ru(1)−Ru(2′)−M(1)	92.81(3)	87.46(19)	90.73(8)	94.2(2)	93
Ru(2)−Ru(1)−Ru(2′)	90.18(4)	93.8(2)	89.88(11)	91.72(16)	86
Ru(2)−M(1)−Ru(2′)	86.67(3)	87.27(11)	88.83(7)	82.87(14)	85

[a] Symmetry transformations used to generate equivalent atoms: $-x + 1, -y, -z + 2$ (for **17**); $-x, -y, -z$ (for **18** and **19**); Ru(2′) = Ru(3) (for **15**), Se(1′) = Se(2) (for **15**). [b] M = W for **15**, **17** and **18**, Mo for **19**.

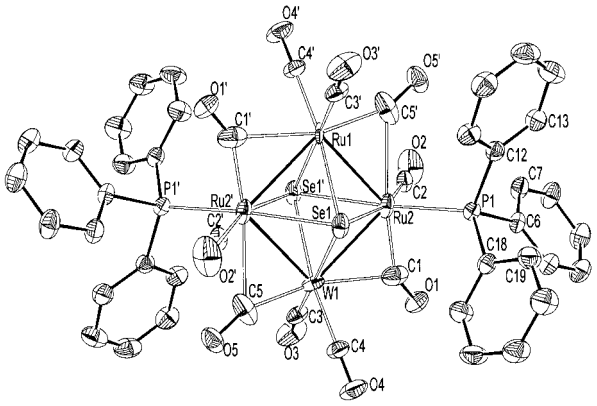

Figure 6. View (ORTEP, 30% probability level) of the molecular structure of one of the two disordered complexes **18** with the atom numbering scheme

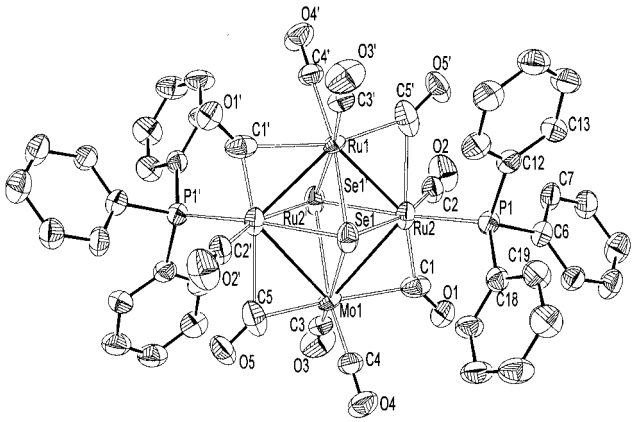

Figure 7. View (ORTEP, 30% probability level) of the molecular structure of one of the two disordered complexes **19** with the atom numbering scheme

seven SEP species. The major optimised bond lengths and angles are given in Table 2. Taking into account that such calculations are known to overestimate the bond lengths between heavy atoms by approximately 2−6%,[15] the optimised geometry of $[WRu_3(\mu_4\text{-Se})_2(\mu\text{-CO})_4(CO)_6(PH_3)_2]$ is in good agreement with the X-ray structures of **15**, **18** and **19**.

Surprisingly, in the case of the reaction between $[W(CO)_3(MeCN)_3]$ and **4**, we obtained the compound $[(CO)_5W(\mu_4\text{-Se})Ru_3(\mu_3\text{-Se})(CO)_7\{P(CH_2Ph)Ph_2\}_2]$ (**20**) as the only isolable product identified by X-ray diffraction methods. It could be considered as the product of a donor-acceptor interaction between a $W(CO)_5$ fragment and a selenido ligand of **10**. The presence of similar products is detectable on the preparative TLC plates in all the growth reactions described above, as red bands attributable to adducts (which decompose during elution) are always observed. In the case of $PPh_2(OMe)$, it was even possible to isolate and recognize, by FT-IR spectroscopy, a cluster analogous to **20**, which, however, rapidly decomposed. The decomposition product was identified as the starting disubstituted *nido* cluster **2**.

A view of cluster **20** is given in Figure 8. A list of the most important bond lengths and angles are given in Table 3.

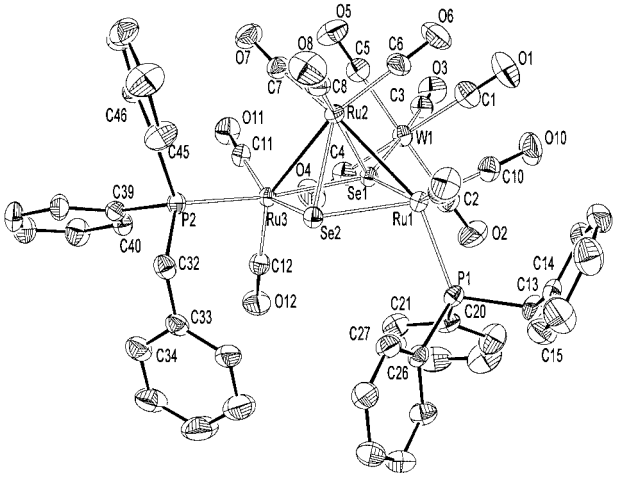

Figure 8. View (ORTEP, 30% probability level) of the molecular structure of **20** with the atom numbering scheme

Table 3. Selected bond lengths (Å) and angles (°) found for compound **20** compared with those calculated for the complex $[(CO)_5W(\mu_4\text{-Se})Ru_3(\mu_3\text{-Se})(CO)_7(PH_3)_2]$

	20	$[(CO)_5W(\mu_4\text{-Se})Ru_3(\mu_3\text{-Se})(CO)_7(PH_3)_2]$
Ru(1)−Ru(2)	2.802(2)	2.907
Ru(2)−Ru(3)	2.8526(13)	2.902
W(1)−Se(1)	2.6852(10)	2.757
Ru(1)−Se(2)	2.5008(15)	2.607
Ru(1)−Se(1)	2.5215(13)	2.582
Ru(2)−Se(2)	2.5379(13)	2.608
Ru(2)−Se(1)	2.5390(12)	2.698
Ru(3)−Se(2)	2.4950(13)	2.618
Ru(3)−Se(1)	2.5203(15)	2.649
Ru(1)−Ru(2)−Ru(3)	87.01(6)	87
Ru(1)−Se(1)−Ru(3)	101.09(5)	100
Ru(1)−Se(2)−Ru(3)	102.38(5)	100
Se(1)−Ru(1)−Se(2)	77.13(5)	81
Se(1)−Ru(3)−Se(2)	78.25(5)	80

It consists of a $[Ru_3(\mu_3\text{-Se})_2(CO)_7\{P(CH_2Ph)Ph_2\}_2]$ moiety linked to a $W(CO)_5$ unit through a coordinative interaction between a selenido ligand and the tungsten atoms [Se1−W1 = 2.685(1) Å]. The $[Ru_3(\mu_3\text{-Se})_2]$ core unit, described as a square pyramid with two ruthenium and two selenium atoms at the base of the pyramid and a ruthenium atom at the apex, is similar to those of **10** and **2** with similar Ru−Ru [2.802(2) and 2.853(1) Å], and Ru−Se bond lengths [ranging from 2.495(1) to 2.539(1) Å]. The two diphenylbenzylphosphane ligands substitute two ruthenium atoms at the base of the pyramid in a *pseudo*-equatorial and *pseudo*-axial position [P1−Ru1 and P2−Ru3 bond lengths of 2.315(1) and 2.345(2) Å]. The quadruply bridging selenido ligand (μ_4-Se) acts as a six-electron donor, two of which serve to attain an 18-electron configuration at the tungsten

atom. An analogous unsubstituted compound of formula $[Os_3(\mu_3\text{-}S)(\mu_4\text{-}S)(CO)_9W(CO)_5]$ was previously reported by Adams et al.[16] In contrast to this osmium derivative, the heptacoordinate Ru2 atom is bound to a carbonyl group essentially *trans* with respect to the (μ_4-Se) ligand [Se1−Ru2−C8 176.9(2)°]. In the parent Os compound the carbonyl group is almost *trans* to the (μ_3-S) ligand [S−Os−C 166.4(2)°] and in that case the better donor character of the μ_3-ligand with respect to the μ_4-ligand has been invoked. In the case of **20** the steric hindrance of the two phosphane ligands predominates over the electronic factors and forces the system to be disposed in the observed way.

As regards the mechanism for the production of **20**, we are far from a unique solution, but it could involve a labile intermediate of formula $[Ru_3(\mu_3\text{-}Se)(\mu_4\text{-}Se)(CO)_7\{P(CH_2Ph)Ph_2\}_2W(CO)_3(CH_3CN)_2]$, formed from $[W(CO)_3(MeCN)_3]$ by loss of one acetonitrile ligand. Subsequently, two MeCN ligands could be substituted by two carbonyls. On the other hand, if the labile intermediate loses two acetonitrile ligands, the anchored $W(CO)_3$ fragment can approach the Ru_2Se_2 basal plane of the pyramid (i.e. the cavity of the *nido* polyhedron), leading to the previously described *closo* clusters. These reaction sequences are depicted in Scheme 4. In the case of $PPh_2(CH_2Ph)$, the corresponding dimetallic *closo* cluster has not been obtained, probably because of the steric hindrance of the benzyl group, which does not facilitate the approach of the $W(CO)_3$ moiety.

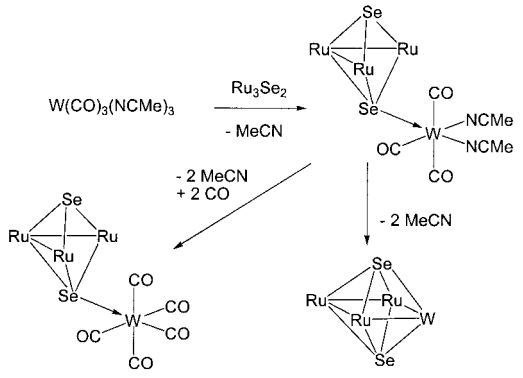

Scheme 4. (Carbonyl groups omitted)

DFT calculations on the $[(CO)_5W(\mu_4\text{-}Se)Ru_3(\mu_3\text{-}Se)(CO)_7(PH_3)_2]$ model (assuming C_1 symmetry) lead to the optimised bond lengths and angles given in Table 3. They are consistent with those computed for $[WRu_3(\mu_4\text{-}Se)_2(\mu\text{-}CO)_4(CO)_6(PH_3)_2]$. It is noteworthy that the computed total energy of $[(CO)_5W(\mu_4\text{-}Se)Ru_3(\mu_3\text{-}Se)(CO)_7(PH_3)_2]$ is 1.1 eV lower than that of $[WRu_3(\mu_4\text{-}Se)_2(\mu\text{-}CO)_4(CO)_6(PH_3)_2]$ + 2CO. Although this value has to be considered as a rough approximation of the enthalpy of the reaction $[(CO)_5W(\mu_4\text{-}Se)Ru_3(\mu_3\text{-}Se)(CO)_7(PH_3)_2] \rightarrow [WRu_3(\mu_4\text{-}Se)_2(\mu\text{-}CO)_4(CO)_6(PH_3)_2]$ + 2CO it is indicative of thermal stability of **20**. However, the adduct compounds are labile and prone to decompose over silica gel in the air in such a way that they cannot be obtained by TLC as mentioned above. Only in the case of $P(CH_2Ph)Ph_2$ were we able to isolate and characterise the corresponding adduct **20**. Moreover, the yield of these adducts, which does not exceed 40%, is influenced by the scarcity of free CO, which could be the limiting factor in the process of formation of the adduct molecules. Adams et al. observed that these adduct species can be prepared by UV irradiation of solutions of $[Os_3(CO)_9(\mu_3\text{-}S)_2]$ and $W(CO)_6$, giving $[Os_3(CO)_9(\mu_3\text{-}S)(\mu_4\text{-}S)\{W(CO)_5\}]$ in 70% yield.[16] This could be a more convenient route to obtain higher yields of similar adducts.

Experimental Section

General Procedures: The starting reagents $[Ru_3(CO)_{12}]$, elemental selenium, phosphanes and Me_3NO are pure commercial products (Aldrich and Fluka) and were used as received. The solvents (C. Erba) were dried and distilled by standard techniques before use. $[Ru_3Se_2(CO)_7(PPh_3)_2]$[2] $M(CO)_3(CH_3CN)_3$ (M = W or Mo)[17] and clusters **8**−**14**[18] were prepared according to literature procedures. All manipulations (prior to the TLC separations) were carried out under dry nitrogen by means of standard Schlenk-tube techniques. Elemental (C, H) analyses were performed with a Carlo Erba EA 1108 automated analyzer. IR spectra (KBr discs or CH_2Cl_2 solutions) were recorded on a Nicolet "Nexus" spectrometer. ^1H (300 MHz) and ^{31}P (162.0 MHz, 85% H_3PO_4 as external reference) NMR spectra ($CDCl_3$ solutions) were recorded on Bruker instruments, AC 300 (^1H) and AMX 400 (^{31}P). NICI Mass spectra (Negative-Ion Chemical Impact) were recorded on a Fennigan MAT SSQ710; *m*/*z* values are reported as the average of the isotopic distributions.

Synthesis of the Phosphane Selenides: The phosphane selenides were obtained as white powders by reacting the corresponding phosphanes with elemental selenium (in excess) in toluene at 90 °C with vigorous stirring. The solutions were dried in vacuo and the residues were extracted with dichloromethane. All products gave satisfactory elemental analysis. Their purity was checked by ^1H NMR spectroscopy.

$Ph_2(PhCH_2)PSe$: Yield 95%. FT-IR (KBr) $\nu_{(P=Se)}$: 526s cm^{-1}. ^{31}P NMR ($CDCl_3$): δ = 34.3 ppm (s, with ^{77}Se satellites, $^1J_{P,Se}$ = 715 Hz).

$Ph_2(MeO)PSe$: Yield 93%. FT-IR (KBr) $\nu_{(P=Se)}$: 520s cm^{-1}. ^{31}P NMR ($CDCl_3$): δ = 88.0 ppm (s, with ^{77}Se satellites, $^1J_{P,Se}$ = 715 Hz).

$(p\text{-}MeO\text{-}C_6H_4)_3PSe$: Yield 97%. FT-IR (KBr) $\nu_{(P=Se)}$: 526s cm^{-1}. ^{31}P NMR ($CDCl_3$): δ = 31.5 ppm (s, with ^{77}Se satellites, $^1J_{P,Se}$ = 718 Hz).

$Ph_2(Me)PSe$: Yield 97%. FT-IR (KBr) $\nu_{(P=Se)}$: 528s cm^{-1}. ^{31}P NMR ($CDCl_3$): δ = 23.3 ppm (s, with ^{77}Se satellites, $^1J_{P,Se}$ = 731 Hz).

Reaction of Phosphane Selenides with $[Ru_3(CO)_{12}]$

Reaction with $Ph_2(MeO)PSe$: $[Ru_3(CO)_{12}]$ (300 mg, 0.47 mmol) was reacted in a 1:2 ratio with $Ph_2(MeO)PSe$ (277 mg, 0.94 mmol) in toluene at 70 °C for 1.5 h in the presence of Me_3NO (35 mg, 0.47 mmol) until the solution turned deep reddish brown. The solvents were evaporated to dryness and the residue was redissolved in a small amount of dichloromethane. TLC separation on silica, using a 2:1 dichloromethane/hexane as eluent, yielded three bands

together with some minor decomposition. The three bands contained clusters $[Ru_3(\mu_3\text{-}Se)_2(CO)_8\{P(OMe)Ph_2\}]$ (orange, **1**; yield 15%), $[Ru_3(\mu_3\text{-}Se)_2(CO)_7\{P(OMe)Ph_2\}_2]$ (red, **2**; yield 30%) and $[Ru_4(\mu_4\text{-}Se)_2(\mu\text{-}CO)_2(CO)_7\{P(OMe)Ph_2\}_2]$ (deep red, **3**; yield 25%) in order of elution.

1: FT-IR (CH_2Cl_2): ν(CO): 2077s, 2045vs, 2027s, 2005s, 1984sh cm^{-1}. ^1H NMR ($CDCl_3$, 298 K): δ = 3.60 (d, $^2J_{H,P}$ = 14.1 Hz, 3 H, CH_3), 7.4−7.9 (m, 10 H, 2Ph) ppm. $^{31}P\{^1H\}$ NMR ($CDCl_3$, 298 K): δ = 140.0 (br. s) ppm. $C_{21}H_{13}O_9PRu_3Se_2$: calcd. C 28.0, H 1.46; found C 27.9, H 1.41.

2: FT-IR (CH_2Cl_2): ν(CO): 2047s, 2015vs, 1973s, 1954sh cm^{-1}. ^1H NMR ($CDCl_3$, 298 K): δ = 3.42 (d), 3.59 (d) and 3.61 (d, $^2J_{H,P}$ = 12.1 Hz, 6 H, CH_3), 7.85−7.20 (m, 20 H, 4Ph) ppm. $^{31}P\{^1H\}$ NMR ($CDCl_3$, 298 K): δ = 146 (s), 141 (s) (isomer B); 139 (br), 137 (br) (isomer A) ppm. $C_{33}H_{26}O_9P_2Ru_3Se_2$: calcd. C 36.4, H 2.41; found C 36.3, H 2.41.

3: FT-IR (CH_2Cl_2): ν(CO): 2041w, 2012vs, 2000s, 1966m, 1844w, 1807w cm^{-1}. ^1H NMR ($CDCl_3$, 298 K): δ = 3.58 and 3.66 (d, $^2J_{H,P}$ = 13.2 Hz, 6 H, CH_3), 7.26−7.64 (m, 20 H, 4Ph). $^{31}P\{^1H\}$ NMR ($CDCl_3$, 298 K): δ = 139 (s) ppm. $C_{35}H_{26}O_{11}P_2Ru_4Se_2$: calcd. C 33.8, H 2.11; found C 33.5, H 2.12.

Reaction with $Ph_2(Me)PSe$: $[Ru_3(CO)_{12}]$ (300 mg, 0.47 mmol) was reacted in a 1:2 ratio with $Ph_2(Me)PSe$ (260 mg, 0.94 mmol) in toluene at 70 °C for 2 h in the presence of Me_3NO (35 mg, 0.47 mmol) until the solution turned deep reddish brown. The solvents were evaporated to dryness and the residue was redissolved in a small amount of dichloromethane. TLC separation on silica gel, using 3:1 dichloromethane/hexane as eluent, yielded four bands: an orange, a red, a brown and a deep red one in order of elution. The four bands contained compounds $[Ru_3(\mu_3\text{-}Se)_2(CO)_8\{P(Me)Ph_2\}]$ (**4**; yield 15%), $[Ru_3(\mu_3\text{-}Se)_2(CO)_7\{P(Me)Ph_2\}_2]$ (**5**; yield 30%), $[Ru_4(\mu_4\text{-}Se)_2(\mu\text{-}CO)_2(CO)_7\{P(Me)Ph_2\}_2]$ (**6**; yield 10%) and $[Ru_4(\mu_4\text{-}Se)_2(\mu\text{-}CO)(CO)_7\{P(Me)Ph_2\}_3]$ (**7**; yield 25%).

4: FT-IR (CH_2Cl_2): ν(CO): 2077s, 2043vs, 2025s, 2066s, 1975m cm^{-1}. ^1H NMR ($CDCl_3$, 298 K): δ = 2.49 (br., 3 H, CH_3), 7.4−7.8 (m, 10 H, 2Ph) ppm. $^{31}P\{^1H\}$ NMR ($CDCl_3$, 298 K): δ = 37.2 (s) ppm. $C_{21}H_{13}O_8PRu_3Se_2$: calcd. C 28.6, H 1.48; found C 28.6, H 1.47.

5: FT-IR (CH_2Cl_2): ν(CO): 2045vs, 2009vs, 1967m, 1946w cm^{-1}. ^1H NMR ($CDCl_3$, 298 K): δ = 2.20 (br), 2.32 (d) and 2.52 (d, $^2J_{H,P}$ = 9.3 Hz, 6 H, CH_3), 7.3−7.7 (m, 20 H, 4Ph) ppm. $^{31}P\{^1H\}$ NMR ($CDCl_3$, 298 K): δ = 52 (s), 43 (s) (isomer B); 47 (br), 40 (br) (isomer A) ppm. $C_{33}H_{26}O_7P_2Ru_3Se_2$: calcd. C 37.6, H 2.48; found C 37.3, H 2.41.

6: FT-IR (CH_2Cl_2): ν(CO): 2056w, 2038w, 2010vs, 1992sh, 1961sh, 1839w, 1800w cm^{-1}. ^1H NMR ($CDCl_3$, 298 K): δ = 2.07 (d) and 2.12 (d, $^2J_{H,P}$ = 9 Hz, 6 H, CH_3), 7.3−7.6 (m, 20 H, 4Ph) ppm. $^{31}P\{^1H\}$ NMR ($CDCl_3$, 298 K): δ = 35.15 (s), 25.1 (s) (3:2). $C_{35}H_{26}O_9P_2Ru_4Se_2$: calcd. C 34.7, H 2.16; found C 34.5, H 2.14.

7: FT-IR (CH_2Cl_2): ν(CO): 2017s, 1995vs, 1984s, 1955m, 1789w cm^{-1}. ^1H NMR ($CDCl_3$, 298 K): δ = 2.02 (d) and 2.30 (d, $^2J_{H,P}$ = 8.4 Hz, 9 H, CH_3), 7.2−7.9 (m, 30 H, 6Ph) ppm. $^{31}P\{^1H\}$ NMR ($CDCl_3$, 298 K): δ = 23.3 (s), 30.0 (s) (2:1). $C_{47}H_{39}O_8P_3Ru_4Se_2$: calcd. C 40.8, H 2.84; found C 40.3, H 2.81.

Synthesis of $[WRu_3(\mu_4\text{-}Se)_2(\mu\text{-}CO)_4(CO)_6\{P(OMe)Ph_2\}_2]$ (15): Compound **2** (50 mg, 0.089 mmol) and $[W(CO)_3(CH_3CN)_3]$ (50 mg, 0.128 mmol) were stirred in dry CH_2Cl_2 for 1 h at room temperature under N_2. The resulting dark solution was evaporated to dryness and the residue was dissolved in CH_2Cl_2 (10 mL). The product (cluster **15**, yield 40%) was separated and purified by TLC on silica gel, using diethyl ether/light petroleum (b.p. 40−60 °C) (2:1) as eluent mixture. FT-IR (CH_2Cl_2): ν(CO): 2043m, 2007vs, 1987vs, 1894m, 1910m, 1831w, 1799w cm^{-1}. ^1H NMR ($CDCl_3$, 298 K): δ = 3.49 (d), 3.58 (d), 3.66 (d) and 3.73 (d, 6 H, $^3J_{H,P}$ = 13.5 Hz, CH_3) (8:4:1:1); 7.10−7.80 (m, 20 H, 4Ph) ppm. $^{31}P\{^1H\}$ NMR ($CDCl_3$, 298 K): δ = 130.0 (s) ppm. MS (NICI): *m/z* (%) = 1356 (95) $[Ru_3W(\mu_4\text{-}Se)_2(CO)_{10}\{P(OMe)Ph_2\}_2]^+$, 1300 (100) $[Ru_3W(\mu_4\text{-}Se)_2(CO)_8\{P(OMe)Ph_2\}_2]^+$, 1272 (42) $[Ru_3W(\mu_4\text{-}Se)_2(CO)_7\{P(OMe)Ph_2\}_2]^+$, 1244 (15) $[Ru_3W(\mu_4\text{-}Se)_2(CO)_6\{P(OMe)Ph_2\}_2]^+$, 1216 (21) $[Ru_3W(\mu_4\text{-}Se)_2(CO)_5\{P(OMe)Ph_2\}_2]^+$, 1188 (16) $[Ru_3W(\mu_4\text{-}Se)_2(CO)_4\{P(OMe)Ph_2\}_2]^+$, 1160 (28) $[Ru_3W(\mu_4\text{-}Se)_2(CO)_3\{P(OMe)Ph_2\}_2]^+$, 1104 (25) $[Ru_3W(\mu_4\text{-}Se)_2(CO)\{P(OMe)Ph_2\}_2]^+$, 1076 (10) $[Ru_3W(\mu_4\text{-}Se)_2\{P(OMe)Ph_2\}_2]^+$. $C_{36}H_{26}O_{12}P_2Ru_3Se_2W$: calcd. C 31.9, H 1.93; found C 31.8, H 2.00.

Synthesis of $[WRu_3(\mu_4\text{-}Se)_2(\mu\text{-}CO)_4(CO)_6\{P(Me)Ph_2\}_2]$ (16): Compound **5** (80 mg, 0.076 mmol) and $[W(CO)_3(CH_3CN)_3]$ (60 mg, 0.153 mmol) were stirred in dry CH_2Cl_2 for 1.5 h at room temperature under N_2. The resulting dark solution was evaporated to dryness and the residue was dissolved in CH_2Cl_2 (10 mL). The product (cluster **16**, yield 45%) was separated and purified by TLC on silica gel, using diethyl ether/light petroleum (b.p. 40−60 °C) (2:1) as eluent mixture. FT-IR (CH_2Cl_2): ν(CO): 2043m, 2007vs, 1978vs, 1894m, 1910m, 1831w, 1800w cm^{-1}. ^1H NMR ($CDCl_3$, 298 K): δ = 2.08 (d), 2.03 (d) and 2.01 (d, $^2J_{H,P}$ = 8.5 Hz, 6 H CH_3) (1:3:9), 7.4−7.5 (m, 20 H, 4Ph) ppm. $^{31}P\{^1H\}$ NMR ($CDCl_3$, 298 K): no observable signals. MS (NICI): *m/z* (%) = 1324 (100) $[Ru_3W(\mu_4\text{-}Se)_2(CO)_{10}\{P(Me)Ph_2\}_2]^+$, 1296 (17) $[Ru_3W(\mu_4\text{-}Se)_2(CO)_9\{P(Me)Ph_2\}_2]^+$, 1268 (38) $[Ru_3W(\mu_4\text{-}Se)_2(CO)_8\{P(Me)Ph_2\}_2]^+$, 1240 (35) $[Ru_3W(\mu_4\text{-}Se)_2(CO)_7\{P(Me)Ph_2\}_2]^+$, 1212 (32) $[Ru_3W(\mu_4\text{-}Se)_2(CO)_6\{P(Me)Ph_2\}_2]^+$, 1184 (31) $[Ru_3W(\mu_4\text{-}Se)_2(CO)_5\{P(Me)Ph_2\}_2]^+$, 1156 (33) $[Ru_3W(\mu_4\text{-}Se)_2(CO)_4\{P(Me)Ph_2\}_2]^+$, 1128 (28) $[Ru_3W(\mu_4\text{-}Se)_2(CO)_3\{P(Me)Ph_2\}_2]^+$, 1100 (20) $[Ru_3W(\mu_4\text{-}Se)_2(CO)_2\{P(Me)Ph_2\}_2]^+$, 1072 (25) $[Ru_3W(\mu_4\text{-}Se)_2(CO\{P(Me)Ph_2\}_2]^+$, 1044 (27) $[Ru_3W(\mu_4\text{-}Se)_2\{P(Me)Ph_2\}_2]^+$. $C_{36}H_{26}O_{10}P_2Ru_3Se_2W$: calcd. C 32.7, H 1.98; found C 32.8, H 2.00.

Synthesis of $[WRu_3(\mu_4\text{-}Se)_2(\mu\text{-}CO)_4(CO)_6\{P(p\text{-}MeO\text{-}C_6H_4)_3\}_2]$ (17): Compound **13** (100 mg, 0.073 mmol) and $[W(CO)_3(CH_3CN)_3]$ (57.3 mg, 0.147 mmol) were stirred in dry CH_2Cl_2 for 1.5 h at room temperature under N_2. The resulting dark solution was evaporated to dryness and the residue was dissolved in CH_2Cl_2 (10 mL). The product (cluster **17**, yield 45%) was separated and purified by TLC on silica gel, using diethyl ether/light petroleum (b.p. 40−60 °C) (2:1) as eluent mixture. FT-IR (CH_2Cl_2): ν(CO): 2039m, 2005vs, 1976s, 1888m, 1831w, 1800w cm^{-1}. ^1H NMR ($CDCl_3$, 298 K): δ = 3.87 (s, 18 H, CH_3), 6.92 (dd, $^3J_{H_\alpha,H_\beta}$ = 9, $^4J_{H_\beta,^{31}P}$ = 1.8 Hz, 12 H, H_βAr), 7.29 (dd, $^3J_{H_\alpha,H_\beta}$ = 9, $^3J_{H_\alpha,^{31}P)}$ = 10.8 Hz, 12 H, H_αAr) ppm. $^{31}P\{^1H\}$ NMR ($CDCl_3$, 298 K): δ = 39.0 (s) ppm. MS (NICI): *m/z* (%) = 1361 (95) $[Ru_3W(\mu_4\text{-}Se)_2(CO)_{10}\{P(p\text{-}MeO\text{-}C_6H_4)_3\}_2]^-$, 1574 (100) $[Ru_3W(\mu_4\text{-}Se)_2(CO)_8\{P(p\text{-}MeO\text{-}C_6H_4)_3\}_2]^+$, 1546 (86) $[Ru_3W(\mu_4\text{-}Se)_2(CO)_7\{P(p\text{-}MeO\text{-}C_6H_4)_3\}_2]^+$, 1518 (72) $[Ru_3W(\mu_4\text{-}Se)_2(CO)_6\{P(p\text{-}MeO\text{-}C_6H_4)_3\}_2]^+$, 1490 (63) $[Ru_3W(\mu_4\text{-}Se)_2(CO)_5\{P(p\text{-}MeO\text{-}C_6H_4)_3\}_2]^+$, 1462 (62) $[Ru_3W(\mu_4\text{-}Se)_2(CO)_4\{P(p\text{-}MeO\text{-}C_6H_4)_3\}_2]^+$, 1432 (43) $[Ru_3W(\mu_4\text{-}Se)_2(CO)_2\{P(p\text{-}MeO\text{-}C_6H_4)_3\}_2]^+$, 1410 (32) $[Ru_3W(\mu_4\text{-}Se)_2(CO\{P(p\text{-}MeO\text{-}C_6H_4)_3\}_2]^+$, 1382 (24) $[Ru_3W(\mu_4\text{-}Se)_2\{P(p\text{-}MeO\text{-}C_6H_4)_3\}_2]^+$. $C_{52}H_{42}O_{16}P_2Ru_3Se_2W$: calcd. C 38.4, H 2.60; found C 38.0, H 2.60.

Mass Spectroscopic data of $[MRu_3(\mu_4\text{-}Se)_2(\mu\text{-}CO)_4(CO)_6(PPh_3)_2]$ [M = W (18), Mo (19)]: The synthesis of the *closo* clusters $[WRu_3(\mu_4\text{-}Se)_2(\mu\text{-}CO)_4(CO)_6(PPh_3)_2]$ (**18**) and $[MoRu_3(\mu_4\text{-}Se)_2(\mu\text{-}CO)_4(CO)_6(PPh_3)_2]$ (**19**) has been reported previously.[12]

18: MS (NICI): *m/z* (%) = 1449 (100) $[Ru_3W(\mu_4\text{-}Se)_2(CO)_{10}\{PPh_3\}_2]^+$, 1421 (20) $[Ru_3W(\mu_4\text{-}Se)_2(CO)_9\{PPh_3\}_2]^+$,

1393 (33) $[Ru_3W(\mu_4\text{-}Se)_2(CO)_8\{PPh_3\}_2]^+$, 1365 (37) $[Ru_3W(\mu_4\text{-}Se)_2(CO)_7\{PPh_3\}_2]^+$, 1337 (31) $[Ru_3W(\mu_4\text{-}Se)_2(CO)_6\{PPh_3\}_2]^+$, 1309 (32) $[Ru_3W(\mu_4\text{-}Se)_2(CO)_5\{PPh_3\}_2]^+$, 1281 (35) $[Ru_3W(\mu_4\text{-}Se)_2(CO)_4\{PPh_3\}_2]^+$, 1253 (22) $[Ru_3W(\mu_4\text{-}Se)_2(CO)_3\{PPh_3\}_2]^+$, 1225 (25) $[Ru_3W(\mu_4\text{-}Se)_2(CO)_2\{PPh_3\}_2]^+$, 1197 (27) $[Ru_3W(\mu_4\text{-}Se)_2(CO)\{PPh_3\}_2]^+$, 1169 (21) $[Ru_3W(\mu_4\text{-}Se)_2\{PPh_3\}_2]^+$. $C_{46}H_{30}O_{10}P_2Ru_3Se_2W$: calcd. C 38.1, H 2.07; found C 38.2, H 2.10.

19: MS (NICI): *m/z* (%) = 1361 (100) $[Ru_3Mo(\mu_4\text{-}Se)_2(CO)_{10}\{PPh_3\}_2]^+$, 1333 (18) $[Ru_3Mo(\mu_4\text{-}Se)_2(CO)_9\{PPh_3\}_2]^+$, 1305 (43) $[Ru_3Mo(\mu_4\text{-}Se)_2(CO)_8\{PPh_3\}_2]^+$, 1277 (41) $[Ru_3Mo(\mu_4\text{-}Se)_2(CO)_7\{PPh_3\}_2]^+$, 1249 (37) $[Ru_3Mo(\mu_4\text{-}Se)_2(CO)_6\{PPh_3\}_2]^+$, 1221 (33) $[Ru_3Mo(\mu_4\text{-}Se)_2(CO)_5\{PPh_3\}_2]^+$, 1193 (22) $[Ru_3Mo(\mu_4\text{-}Se)_2(CO)_4\{PPh_3\}_2]^+$, 1165 (34) $[Ru_3Mo(\mu_4\text{-}Se)_2(CO)_3\{PPh_3\}_2]^+$, 1137 (18) $[Ru_3Mo(\mu_4\text{-}Se)_2(CO)_2\{PPh_3\}_2]^+$, 1109 (31) $[Ru_3Mo(\mu_4\text{-}Se)_2(CO)\{PPh_3\}_2]^+$, 1081 (23) $[Ru_3Mo(\mu_4\text{-}Se)_2\{PPh_3\}_2]^+$. $C_{46}H_{30}MoO_{10}P_2Ru_3Se_2$: calcd. C 40.5, H 2.20; found C 40.6, H 2.22.

Synthesis of the Adduct $[(CO)_5W(\mu_4\text{-}Se)Ru_3(\mu_3\text{-}Se)(CO)_7\{P(CH_2Ph)Ph_2\}_2]$ (20): Compound **10** (100 mg, 0.083 mmol) and $[W(CO)_3(CH_3CN)_3]$ (65 mg, 0.166 mmol) were stirred in dry CH_2Cl_2 for 1 h at room temperature under N_2. The resulting dark solution was evaporated to dryness and the residue was dissolved in CH_2Cl_2 (10 mL). The product (cluster **20**, yield 40%) was separated and purified by TLC on silica gel, using dichloromethane/light petroleum (b.p. 40−60 °C) (1:1) as eluent. FT-IR (CH_2Cl_2): ν(CO): 2071m, 2050vs, 2022vs, 1987m, 1972m, 1931s, 1895w cm^{-1}. ^1H NMR: δ = 3.81 (br., 4 H, CH_2 Bz), 7.7−6.5 (m, 24 H, Ph) ppm. $^{31}P\{^1H\}$ NMR: δ = 43.5 (br.) ppm. $C_{50}H_{34}O_{12}P_2Ru_3Se_2W$: calcd. C 39.2, H 2.24; found C 39.1, H 2.23.

Crystal Structure Determination of 2, 10, 15, 17, 18, 19 and 20·2CH_2Cl_2: Suitable crystals for the X-ray analysis for all complexes were obtained by layering methanol on dichloromethane solutions. The intensity data, at room temperature, of **2**, **10** and **20·2CH_2Cl_2** were collected on a Bruker AXS Smart 1000 single crystal diffractometer (equipped with an area detector using a graphite monochromated Mo-K_α radiation, λ = 0.71073 Å), those of **15**, **17**, and **18** on a Philips PW 1100 single-crystal diffractometer (graphite monochromated Mo-K_α radiation, λ = 0.71073 Å) and those of **19** on an Enraf Nonius CAD 4 single-crystal diffractometer (graphite monochromated Cu-K_α radiation, λ = 1.54184 Å). Crystallographic and experimental details for the structures are summarised in Table 4. An empirical correction for absorption was made for **15**, **17**, **18** and **19** [maximum and minimum value for the transmission coefficient was 1.000 and 0.7262 (**15**), 1.000 and 0.6872 (**17**), 1.000 and 0.5947 (**18**) and 1.000 and 0.460 (**19**)].[19a,19b] For complexes **2**, **10** and **20·2CH_2Cl_2** [maximum and minimum effective transmission value was 1.000 and 1.000 (**2**), 1.000 and 0.8532 (**10**) and 1.000 and 0.5104 (**20·2CH_2Cl_2**)] the raw frame data were processed using SAINT and SADABS to yield the reflection data file and the Bruker software was used for the absorption correction.[19c−19e] The structures were solved by Patterson and Fourier methods and refined by full-matrix least-squares procedures (based on F_o^2) (SHELX-97)[20] first with isotropic thermal parameters and then with anisotropic thermal parameters in the last cycles of refinement for all the non-hydrogen atoms. In the crystals of **20** dichloromethane molecules of solvation were found. The hydrogen atoms were introduced into the geometrically calculated positions and refined as riding on the corresponding parent atoms.

In the crystals of **17**, **18** and **19** a disorder exists which involves the mutually opposite Ru and W atoms of the *closo* core of the cluster, resulting in a disordered $[Ru_3M(\mu_4\text{-}Se)_2]$ core, distributed in two positions with the same occupancy factor, instead of the centrosymmetric $[M_2Ru_2(\mu_4\text{-}Se)_2]$ core.

CCDC-208915 (**2**), -208916 (**10**), -208917 (**15**), -208920 (**17**), -208918 (**18**), -208919 (**19**) and -208921 (**20·2CH_2Cl_2**) contain the supplementary crystallographic data for this paper. These data can be obtained free of charge at www.ccdc.cam.ac.uk/conts/retrieving.html [or from the Cambridge Crystallographic Data Centre, 12, Union Road, Cambridge CB2 1EZ, UK; Fax: (internat.) +44-1223/336-033; E-mail: deposit@ccdc.cam.ac.uk].

Table 4. Crystal data and structure refinement for **2**, **10**, **15**, **17**, **18**, **19** and **20·2CH_2Cl_2**

	2	**10**	**15**	**17**	**18**	**19**	**20·2CH_2Cl_2**
Formula	$C_{33}H_{26}O_9P_2Ru_3Se_2$	$C_{45}H_{34}O_7P_2Ru_3Se_2$	$C_{36}H_{26}O_{12}P_2Ru_3Se_2W$	$C_{52}H_{42}O_{16}P_2Ru_3Se_2W$	$C_{46}H_{30}O_{10}P_2Ru_3Se_2W$	$C_{46}H_{30}MoO_{10}P_2Ru_3Se_2$	$C_{52}H_{38}Cl_4O_{12}P_2Ru_3Se_2W$
Mol. wt.	1089.61	1209.79	1357.49	1629.78	1449.62	1361.71	1703.54
Crystal system	triclinic	triclinic	monoclinic	monoclinic	triclinic	triclinic	triclinic
Space group	$P\bar{1}$	$P\bar{1}$	$P2_1/n$	$P2_1/c$	$P\bar{1}$	$P\bar{1}$	$P\bar{1}$
a (Å)	8.792(3)	11.804(5)	14.533(4)	12.054(3)	10.102(5)	10.229(5)	13.819(3)
b (Å)	10.701(4)	14.109(5)	29.729(5)	15.643(5)	11.156(5)	11.147(5)	18.333(5)
c (Å)	21.163(5)	14.885(5)	9.572(3)	14.458(4)	11.205(5)	11.151(5)	13.259(3)
α (°)	79.90(5)	65.23(5)	90	90	95.86(2)	95.56(2)	77.36(5)
β (°)	85.36(5)	77.34(5)	98.76(5)	94.29(5)	97.33(2)	97.55(2)	66.38(5)
γ (°)	71.63(5)	72.54(5)	90	90	110.16(2)	110.29(2)	80.49(5)
V ($Å^3$)	1860(1)	2135(1)	4087(1)	2719(1)	1161(1)	1168(1)	2992(1)
Z	2	2	4	2	1	1	2
D_{calcd} (g cm^{-3})	1.946	1.882	2.206	1.991	2.073	1.935	1.891
F(000)	1052	1180	2568	1572	690	658	1636
Crystal size	0.11 × 0.12 × 0.20	0.18 × 0.22 × 0.25	0.15 × 0.21 × 0.19	0.12 × 0.15 × 0.11	0.14 × 0.31 × 0.15	0.12 × 0.21 × 0.09	0.22 × 0.11 × 0.20
μ, cm^{-1}	32.96	28.79	58.11	43.92	51.18	127.59	41.64
Reflns. collected	19813	8705	7629	5945	5606	4393	43030
Reflns. unique	9941 (R_{int} = 0.0545)	7003 (R_{int} = 0.0527)	7183 (R_{int} = 0.0456)	5945 (R_{int} = 0.0245)	5606 (R_{int} = 0.000)	4393 (R_{int} = 0.000)	16317 (R_{int} = 0.0690)
Obs. reflns. [$I > 2\sigma(I)$]	5117	3367	5539	3914	4072	2991	9452
R indices[a]	*R*1 = 0.0436	*R*1 = 0.0416	*R*1 = 0.0480	*R*1 = 0.0372	*R*1 = 0.0588	*R*1 = 0.0634	*R*1 = 0.0395
[$I > 2\sigma(I)$]	*wR*2 = 0.0754	*wR*2 = 0.0684	*wR*2 = 0.1229	*wR*2 = 0.0943	*wR*2 = 0.1248	*wR*2 = 0.1718	*wR*2 = 0.0882
R indices (all data)	*R*1 = 0.1152	*R*1 = 0.1129	*R*1 = 0.0671	*R*1 = 0.0719	*R*1 = 0.0847	*R*1 = 0.0936	*R*1 = 0.0946
	*wR*2 = 0.0927	*wR*2 = 0.0823	*wR*2 = 0.1386	*wR*2 = 0.1145	*wR*2 = 0.1405	*wR*2 = 0.2210	*wR*2 = 0.1034

[a] $R1 = \Sigma||F_o| - |F_c||/\Sigma|F_o|$; $wR2 = \{\Sigma[w(F_o^2 - F_c^2)^2]/\Sigma[w(F_o^2)^2]\}^{1/2}$.

Computational Details: Density functional theory (DFT) calculations were carried out using the Amsterdam density functional (ADF) program[21] developed by Baerends and co-workers.[22] The Vosko−Wilk−Nusair parameterization[23] was used for the local density approximation (LDA) with gradient correction for exchange (Becke88)[24] and correlation (Perdew86).[25] Relativistic corrections were added using the ZORA (Zeroth Order Regular Approximation) scalar Hamiltonian.[26] The atom electronic configurations were described by a triple-ξ Slater-type orbital (STO) basis set for H 1s, C, O 2s and 2p, P 3s and 3p and Se 4s and 4p augmented with a 3d single-ξ polarisation function for C, O, P, with a 2p single-ξ polarisation function for H and 4d single-ξ polarisation function for Se. A triple-ξ STO basis set was used for Mo, Ru 4d and 5s and for W 5d and 6s augmented with a single-ξ 5p for Mo and Ru and 6p for W. A double-ξ STO basis set was used for W 5s and 5p. A frozen-core approximation was used to treat the core electrons of C, O, P, Se, Mo, Ru and W.

Acknowledgments

Financial support from Ministero dell'Università e della Ricerca Scientifica e Tecnologica (Cofin 2000) is gratefully acknowledged. The facilities of the Centro Interfacoltà di Misure "G. Casnati" (Università di Parma) were used to record the NMR and mass spectra. Computing facilities were provided by the Centre de Ressources Informatiques (CRI) of Rennes and the Institut de Développement et de Ressources en Informatique Scientifique du Centre National de la Recherche Scientifique (IDRIS-CNRS).

[1] D. Cauzzi, C. Graiff, G. Predieri, A. Tiripicchio, in *Metal Clusters in Chemistry* (Eds.: P. Braunstein, L. Oro, P. Raithby), vol. 1, VCH, Weinheim **1999**, 193.
[2] P. Baistrocchi, D. Cauzzi, M. Lanfranchi, G. Predieri, A. Tiripicchio, M. Tiripicchio Camellini, *Inorg. Chim. Acta* **1995**, *235*, 173.
[3] D. Cauzzi, C. Graiff, C. Massera, G. Predieri, A. Tiripicchio, D. Acquotti, *J. Chem. Soc., Dalton Trans.* **1999**, 3515.
[4] D. Cauzzi, C. Graiff, M. Lanfranchi, G. Predieri, A. Tiripicchio, *J. Chem. Soc., Dalton Trans.* **1995**, 2321.
[5] D. Cauzzi, C. Graiff, C. Massera, G. Predieri, A. Tiripicchio, *Inorg. Chim. Acta* **2000**, *300−302*, 471.
[6] D. Cauzzi, C. Graiff, C. Massera, G. Predieri, A. Tiripicchio, *J. Cluster Sci.* **2001**, *12*, 259.
[7] D. Cauzzi, C. Graiff, C. Massera, G. Predieri, A. Tiripicchio, *Eur. J. Inorg. Chem.* **2001**, 721.
[8] P. Braunstein, J. Rosé, Heterometallic Clusters in Catalysis, in *Metal Clusters in Chemistry* (Eds.: P. Braunstein, L. A. Oro, P. R. Raithby), VCH, Weinheim, **1999**, pp. 616−677.
[9] P. Braunstein, E. Sappa, A. Tiripicchio, *Coord. Chem. Rev.* **1985**, *65*, 219.
[10] [10a] C. Graiff, A. Ienco, C. Massera, C. Mealli, G. Predieri, A. Tiripicchio, F. Ugozzoli, *Inorg. Chim. Acta* **2002**, *330*, 95. [10b] P. Braunstein, C. Graiff, C. Massera, G. Predieri, J. Rosé, A. Tiripicchio, *Inorg. Chem.* **2002**, *41*, 1372.
[11] R. D. Adams, T. A. Wolfe, W. Wu, *Polyhedron* **1991**, *10*, 447.
[12] D. Cauzzi, C. Graiff, C. Massera, G. Mori, G. Predieri, A. Tiripicchio, *J. Chem. Soc., Dalton Trans.* **1998**, 321.
[13] D. Cauzzi, C. Graiff, M. Lanfranchi, G. Predieri, A. Tiripicchio, *J. Organomet. Chem.* **1997**, *536−537*, 497.
[14] D. Cauzzi, C. Graiff, G. Predieri, A. Tiripicchio, C. Vignali, *J. Chem. Soc., Dalton Trans.* **1999**, 237.
[15] M. T. Garland, J.-F. Halet, J.-Y. Saillard, *Inorg. Chem.* **2001**, *40*, 3342.
[16] R. D. Adams, I. T. Horvath, S. Wang, *Inorg. Chem.* **1985**, *24*, 1728.
[17] H. Werner, K. Dechelmann, U. Schoenenbergher, *Helv. Chim. Acta* **1970**, *53*, 2002.
[18] D. Belletti, D. Cauzzi, C. Graiff, A. Minarelli, R. Pattacini, G. Predieri, A. Tiripicchio, *J. Chem. Soc., Dalton Trans.* **2002**, 3160.
[19] [19a] N. Walker, D. Stuart, *Acta Crystallogr., Sect. A* **1983**, *39*, 158. [19b] F. Ugozzoli, *Comput. Chem.* **1987**, *11*, 109. [19c] *SMART Software Users Guide, Version 5.0*; Bruker Analytical X-ray Systems, Madison, WI, **1999**. [19d] *SAINT Software Users Guide*; Bruker Analytical X-ray Systems, Madison, WI, **1999**. [19e] G. M. Sheldrick, *SADABS*, Bruker Analytical X-ray Systems, Madison, WI, **1999**.
[20] [20a] G. M. Sheldrick, *SHELXL-93*, a program for crystal structure determination; University of Göttingen, Germany, **1993**. [20b] G. M. Sheldrick, *SHELXL-97, Program for crystal structure refinement*; University of Göttingen, Germany, **1997**.
[21] Amsterdam Density Functional program (ADF, 2000.02); Division of Theoretical Chemistry, Vrije Universiteit, De Boelelaan 1083, 1081 HV Amsterdam, The Netherlands; http://www.scm.com.
[22] [22a] E. J. Baerends, D. E. Ellis, P. Ros, *Chem. Phys.* **1973**, *2*, 41. [22b] E. J. Baerends, P. Ros, *Int. J. Quantum Chem.* **1978**, *S12*, 169. [22c] P. M. Boerringter, G. te Velde, E. J. Baerends, *Int. J. Quantum Chem.* **1988**, *33*, 87. [22d] G. te Velde, E. J. Baerends, *Int. J. Quantum Chem.* **1992**, *99*, 84.
[23] S. H. Vosko, L. Wilk, M. Nusair, *Can. J. Phys.* **1980**, *58*, 1200.
[24] [24a] A. D. Becke, *J. Chem. Phys.* **1986**, *84*, 4524. [24b] A. D. Becke, *Phys. Rev. A* **1988**, *38*, 3098.
[25] J. P. Perdew, *Phys. Rev. B* **1986**, *33*, 8822.
[26] [26a] E. van Lenthe, E. J. Baerends, J. G. Snijders, *J. Chem. Phys.* **1993**, *99*, 4597. [26b] E. van Lenthe, E. J. Baerends J. G. Snijders, *J. Chem. Phys.* **1994**, *101*, 9783. [26c] E. van Lenthe, R. van Leeuwen, E. J. Baerends, *Int. J. Quantum Chem.* **1996**, *57*, 281. [26d] E. van Lenthe, E. J. Baerends, J. G. Snijders, *J. Chem. Phys.* **1996**, *105*, 6505. [26e] E. van Lenthe, A. Ehlers, E. J. Baerends, *J. Chem. Phys.* **1999**, *110*, 8943.

Received June 21, 2003
Early View Article
Published Online February 3, 2004

